Study on the Synergistic Corrosion Inhibition Effect between Sodium Silicate and Triethanolamine for 45 Steel Corrosion in 3.5% NaCl solution

Chuanbin Li[1,2], Zhiqiang Sun[1,2], Mingjie Kang[1,2], Zhenwei Yan[1,2,], Zhaojun Tan[1,2], Quande Li[3,4,*], Wen Wang[1], Mingqi Tang[5], Gang Li[1], Zaiqiang Feng[5], Yuguo Gao[1,2]*

[1] School of Mechanical Engineering, North China University of Water Resources and Electric Power, Zhengzhou 450011, PR China
[2] Henan International Joint Laboratory of Thermo-Fluid Electro-Chemical System for New Energy Vehicle, Zhengzhou 450011, PR China
[3] State Key Laboratory of Long-life High Temperature Materials, Deyang 618000, PR China
[4] Dongfang Turbine Co LTD, Deyang 618000, PR China
[5] School of Materials Science and Engineering, North China University of Water Resources and Electric Power, Zhengzhou 450011, PR China
E-mail: yanzhenwei@163.com (Z. Yan), 13603990078@163.com (Z. Tan), quandelee@126.com (Q. Li)

Silicate is an environment-friendly corrosion inhibitor with abundant resources and low cost. Given the shortcomings of protective films formed by silicate corrosion inhibitors and their short protection duration, the formation of a composite corrosion inhibitor comprising sodium silicate as the base solution and triethanolamine was investigated using 45 steel as the substrate. Humidity and temperature accelerated corrosion testing, scanning electron microscopy and laser confocal microscopy, electrochemical testing and molecular simulation were used to determine the effect of triethanolamine on the corrosion inhibition performance of sodium silicate, revealing a synergistic adsorption phenomenon. Molecular simulation verified the synergistic corrosion inhibitory mechanism of sodium silicate and triethanolamine. The results showed that the presence of triethanolamine could improve the corrosion inhibition performance of sodium silicate due to the synergistic adsorption effect of triethanolamine and sodium silicate. Since there was also a competitive adsorption relationship between the two components, when the amount of triethanolamine exceeded 3 g·L^{-1} the corrosion inhibition effect of the composite corrosion inhibitor began to decrease. Therefore, the corrosion inhibitor with sodium silicate at 10 g·L^{-1} and triethanolamine at 3 g·L^{-1} had the best synergistic corrosion inhibitory effect.

1. INTRODUCTION

Corrosion inhibitor protection technologies—substances that can slow down or completely prevent metal corrosion—are widely used to prevent corrosion. Their advantages include low dosage, quick effect, low cost and convenience of use[1,2,3]. Currently, the development of high-efficiency composite corrosion inhibitors that are environmentally friendly and low cost has become the focus and challenge in this field[4,5]. Silicate is abundant, non-toxic, benign and low in cost and does not breed bacteria; it is an 'environmentally friendly' corrosion inhibitor. Sodium silicate is the most common type of silicate corrosion inhibitor. Atik[6] prepared a complete and transparent SiO_2 sol film on a metal surface, with scanning electron microscopy (SEM) revealing that the film on the surface of the metal has defects but maintained some anti-corrosion effect. As deposited protective films formed by silicate are porous, the corrosion inhibitory effect of silicate alone is poor. It has been reported[7] that when the concentration of sodium silicate was 100 $mg \cdot L^{-1}$, the corrosion rate was 0.322 $mm \cdot a^{-1}$, while the corrosion rate without any corrosion inhibitor under the same conditions was 0.477 $mm \cdot a^{-1}$. These results show that the effect of sodium silicate alone as a corrosion inhibitor is not ideal. Therefore, when used as a corrosion inhibitor, silicate needs to be combined with other corrosion inhibitors to improve its corrosion inhibitory effect[8].

Triethanolamine is a low-cost, environmentally friendly organic corrosion inhibitor that is widely used in a variety of composite corrosion inhibitors[9,10]. In the present study, sodium silicate was used as the base solution and triethanolamine was added in different proportions to prepare a composite corrosion inhibitor. The influence of triethanolamine on the corrosion inhibition performance of sodium silicate was determined using humidity and temperature accelerated corrosion testing, SEM and laser confocal microscopy and electrochemical testing. Molecular dynamics simulation was also used to further reveal the synergistic corrosion inhibitory mechanism of sodium silicate and triethanolamine.

2. EXPERIMENTAL

2.1. Inhibitor and sample preparation

Sodium silicate (SS) (10 g) was completely dissolved in distilled water (1 L) with stirring at room temperature. The appropriate amount of triethanolamine (TEA) was added to this solution with thorough stirring to obtain triethanolamine concentrations of 1, 2, 3, 4, 5 and 6 $g \cdot L^{-1}$ composite corrosion inhibitor solutions. The substrate material was 45 steel, the main components are shown in Table 1.

Table 1. Main components of 45 steel

element	C	Si	Mn	S	P	Cr	Ni	Cu
content%	0.42~0.50	0.17~0.37	0.5~0.8	≤0.035	≤0.035	≤0.25	≤0.30	≤0.25

The metal samples were cut into rectangular parallelepipeds that were 80 mm long, 60 mm wide and 3 mm thick. The samples were polished with sandpaper from coarse to fine to obtain a surface roughness of 0.4–0.2. Then, ultrasonic cleaning was conducted in acetone and anhydrous ethanol, three

times each sequentially, to remove surface oil, stains and sands. Finally, the samples were dried for later use.

2.2. Humidity and temperature acceleration test

The prepared metal samples were immersed slowly and vertically in either the sodium silicate corrosion inhibitor or the composite corrosion inhibitor with different ratios of triethanolamine and sodium silicate. One minute later, the samples were slowly removed vertically and dried at room temperature for 2 hours. The resulting samples and samples without corrosion inhibitors were placed vertically in a humidity and temperature chamber at 80 ± 1 °C and relative humidity of 95%. During the humidity and temperature accelerated corrosion test, the chamber was every 24 hours to observe the surface of the samples. At the end of the test, the samples were removed from the chamber, allowed to dry and the surface corrosion morphology was observed.

2.3. Electrochemical measurement

Electrochemical testing was carried out on the Chenhua CHI760E electrochemical workstation using a three-electrode system. The uncoated sample or the samples coated with different inhibitors were used as the working electrode, a platinum plate as the auxiliary electrode, KCl saturated calomel electrode (SCE) as the reference electrode and 3.5% NaCl solution as the electrolyte. The open-circuit potential, polarisation curve and electrochemical impedance were measured. The open-circuit potential test time was set to 180 s to obtain a steady open circuit potential. The electrochemical impedance test potential was at the open circuit potential and the AC signal frequency range was 0.01–100 kHz. The potentiodynamic polarisation measurement scan rate was 5 mV·s^{-1} and the potential range was ± 0.5 V (vs. SCE) of the open circuit potential.

3. RESULTS AND DISCUSSION

3.1. Corrosion behavior under accelerated corrosion

It can be seen from Figure 1 that the surface corrosion of the sample without inhibitor was the most pronounced (Figure 1(a)). The surface corrosion of the sample coated with sodium silicate corrosion inhibitor was significantly improved compared to the sample without corrosion inhibitor but there were still many corrosion marks (Figure 1(b)). Although the sodium silicate film provided some corrosion inhibitory effect [11], it could not protect the sample for long. The composite corrosion inhibitors formed by adding different concentrations of triethanolamine solution to the sodium silicate solution had significantly better anti-corrosion effects than the sodium silicate corrosion inhibitor (Figure 1(c)–(h).
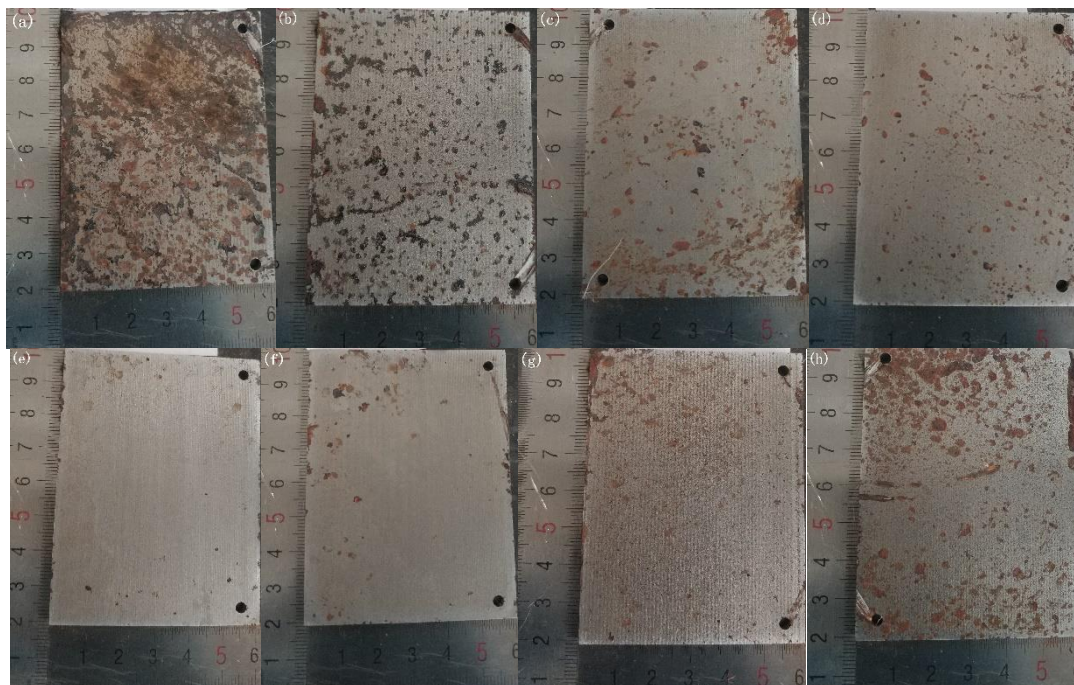
Figure 1. Macroscopical photographs of the samples following the temperature and humidity accelerated corrosion test at 80 ± 1 °C and relative humidity of 95% for 240 h: (a) blank sample; (b) sample coated with sodium silicate; sample coated with sodium silicate and triethylamine at (c) 1 g·L^{-1}; (d) 2 g·L^{-1}; (e) 3 g·L^{-1}; (f) 4 g·L^{-1}; (g) 5 g·L^{-1} and (h) 6 g·L^{-1}.

As the amount of triethanolamine increased, the corrosion inhibitory effect of the composite corrosion inhibitor was more pronounced and the corrosion on the surface of the sample gradually decreased. When the concentration of triethanolamine reached 3 g·L^{-1}, the surface had virtually no corrosion marks and the corrosion inhibitory effect was optimal (Figure 1(e)). However, as the addition of triethanolamine continued to increase, the corrosion inhibitory effect of the composite corrosion inhibitor gradually worsened. When the concentration of triethanolamine reached 6 g·L^{-1} (Figure 1(h)), the number and area of corrosion marks on the surface of the sample were similar to those observed for the sample coated with sodium silicate inhibitor. The reason for this phenomenon was that, when the concentration of triethanolamine was low, the protective film formed by the composite inhibitor still had defects and large areas of corrosion appeared on the surface of the sample. As the concentration of triethanolamine increased, the protective film gradually compacted and became more uniform, leading to a decrease in corrosion that was optimal at a triethanolamine concentration of 3 g·L^{-1}. However, as the concentration of triethanolamine further increased, the corrosion inhibitory effect of the composite corrosion inhibitor gradually deteriorated. This was because the combination of triethanolamine and sodium silicate resulted in a synergistic corrosion inhibition effect; that is, an enhanced corrosion inhibitory effect by the use of two or more corrosion inhibitors[12,13]. This synergism was not simply due to an additive effect; rather, it was the result of mutual promotion. Therefore, when the amount of triethanolamine reached 3 g·L^{-1}, the synergistic effect of corrosion inhibition was optimal. As the amount of triethanolamine further increased, an antagonistic effect appeared whereby the combination of the two corrosion inhibitors resulted in a decreased corrosion inhibitory effect.

To further study the formation of the protective films, SEM, optical microscopy and laser confocal microscopy were used to observe the blank sample, the sample coated with sodium silicate inhibitor and the samples coated with composite inhibitor comprising different amounts of triethanolamine. The results are shown in Figure 2.
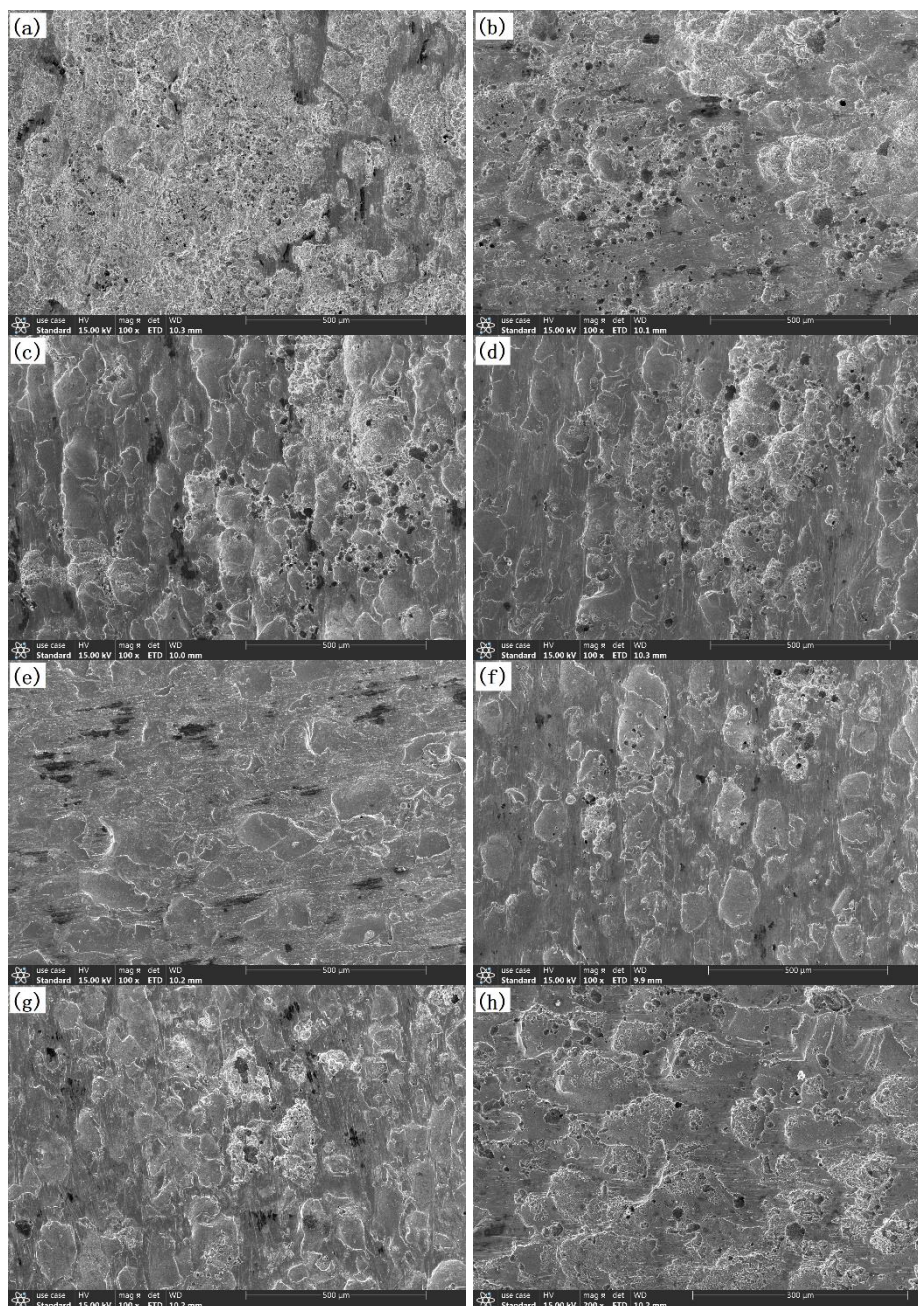
Figure 2. SEM images of the samples from the temperature and humidity accelerated corrosion test at 80 ± 1 °C and relative humidity of 95% for 240 h: (a) blank sample; (b) sample coated with sodium silicate; sample coated with sodium silicate and triethylamine at (c) 1 g·L^{-1}; (d) 2 g·L^{-1}; (e) 3 g·L^{-1}; (f) 4 g·L^{-1}; (g) 5 g·L^{-1} and (h) 6 g·L^{-1}.

It can be observed from Figure 2(a) that the surface of the blank sample was seriously corroded and covered with porous cellular corrosion products after the humidity and temperature accelerated corrosion test. This was because there was no protective film on the surface. Figure 2(b) shows the surface morphology of the 45 steel coated with sodium silicate corrosion inhibitor following humidity and temperature accelerated corrosion. The sample surface was less corroded than that of the blank sample, with less porous cellular corrosion products. Additionally, although the surface of the sample was not completely covered with cellular corrosion products, the intrusion of hot and humid air through defects in the sodium silicate surface film left many tiny holes on the surface of the sample. This phenomenon has been extensively reported in the literature[14,15], which suggested that a thin film of silica formed as sodium silicate dissolved on the surface of the samples and adsorbed tightly on the surface of the sample to prevent corrosion.
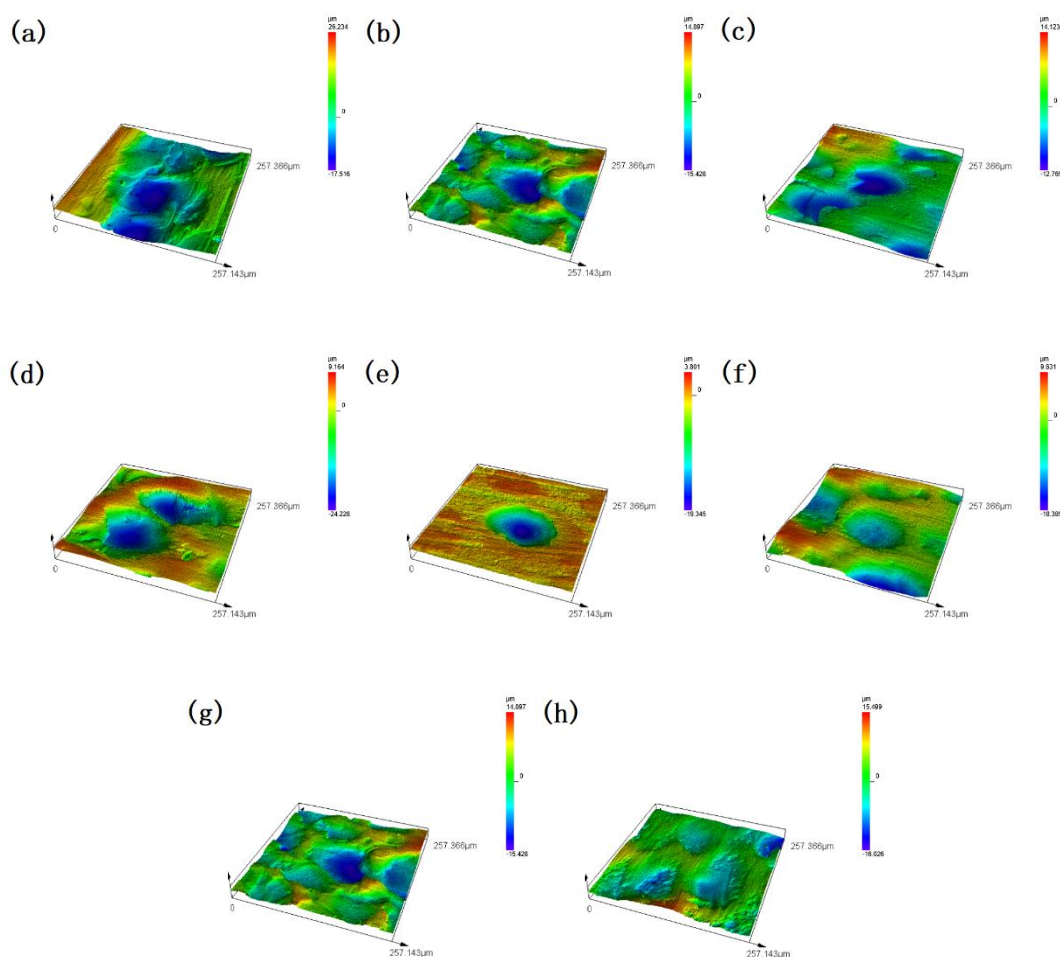
Figure 3. Laser confocal images of the samples following the temperature and humidity accelerated corrosion test at 80 ± 1 °C and relative humidity of 95% for 240 h: (a) blank sample; (b) sample coated with sodium silicate; sample coated with sodium silicate and triethylamine at (c) 1 g·L^{-1}; (d) 2 g·L^{-1}; (e) 3 g·L^{-1}; (f) 4 g·L^{-1}; (g) 5 g·L^{-1} and (h) 6 g·L^{-1}.

Figures 2(c), (d) and (e) show the surface morphology of 45 steel coated with the composite inhibitors containing 1, 2 and 3 $g \cdot L^{-1}$ triethanolamine, respectively, following humidity and temperature accelerated corrosion testing. When the amount of triethanolamine was 1 $g \cdot L^{-1}$, there were considerably fewer corrosion products and pores in the sample surface compared to the samples without corrosion inhibitor and with sodium silicate corrosion inhibitor. As the amount of triethanolamine increased, the number of corrosion products and surface pores gradually decreased. When the amount of triethanolamine reached 3 $g \cdot L^{-1}$, there were no obvious corrosion products or pores on the surface of the sample. When the addition amount of triethanolamine reaches 4 $g \cdot L^{-1}$ (Figure 2(f)), corrosion products began to appear on the surface of the sample again. As the amount of triethanolamine further increased (Figure 2(g) and (h)), the corrosion products on the surface of the sample also increased but to a significantly lesser extent than for the samples without corrosion inhibitor and with sodium silicate corrosion inhibitor. This indicated that the protective film formed by the composite corrosion inhibitor was relatively intact. After 240 hours of humidity and temperature accelerated corrosion, the protective film was only slightly damaged. Therefore, the corrosion inhibitory effect of the triethanolamine composite corrosion inhibitor was markedly better than that of the sodium silicate corrosion inhibitor, alone.

Laser confocal microscopy was used to analyse the corrosion morphology of the different samples. It can be observed from Figure 3(a) that the surface of the sample without any corrosion inhibitor was covered by rough corrosion products, indicating that the surface of the sample was severely corroded. It can be observed from Figure 3(b) that the difference in the surface levels of the sample coated with sodium silicate corrosion inhibitor was smaller than that in Figure 3(a), indicating that the sodium silicate corrosion inhibitor had a certain corrosion inhibitory effect on the 45 steel sample. Figures 3(c), (d) and (e) show the results for the 45 steel coated by the composite inhibitor with 1, 2 and 3 $g \cdot L^{-1}$ triethylamine, respectively. When 1 $g \cdot L^{-1}$ triethanolamine was added, the surface became significantly flatter and, as the amount of triethanolamine in the composite corrosion inhibitor increased, the surface of the sample became increasingly flat. At 3 $g \cdot L^{-1}$ triethanolamine, the surface of the sample contained a few small protrusions, holes and corrosion marks but was generally flat. When the amount of triethanolamine reached 4 $g \cdot L^{-1}$, increased corrosion products began to appear on the surface of the sample. As the amount of triethanolamine further increased (Figure 3(f) and (g)), the corrosion products on the surface of the sample continuously increased and the surface became more uneven; however, the level differences were still significantly less than for the uncoated sample or the sample coated just with sodium silicate corrosion inhibitor. This showed that the protective film formed by the composite corrosion inhibitor was relatively complete. After 240 hours of humidity and temperature accelerated corrosion testing, the protective film was only slightly damaged. Therefore, the corrosion inhibitory effect of the composite corrosion inhibitor was markedly better than that of the sodium silicate corrosion inhibitor.

The results of the humidity and temperature accelerated corrosion experiment showed that the use of either sodium silicate alone or the combination of sodium silicate and triethanolamine had a significant corrosion inhibitory effect on 45 steel. The corrosion inhibitory effect of the composite corrosion inhibitor was significantly greater than that of the sodium silicate corrosion inhibitor. Furthermore, rather than the more triethanolamine the better, it was found that there was an optimal

amount. This result was consistent with the theory of synergistic adsorption[16,17]. This [18] states that, when there is only one type of corrosion inhibitor in solution, there is only one kind of interaction between the corrosion inhibitor molecules in the corrosion inhibitor film. When the solution contains two types of corrosion inhibitors in appropriate concentrations, there will be interactions between their different molecules in the film. If the strength of the interaction between different molecules is greater than the strength of the interaction between the same molecules, the corrosion inhibitor film formed by the different molecules will be denser, thereby improving the performance of the composite corrosion inhibitor. But when the concentration of one of the two corrosion inhibitors is too high, there will competitive adsorption of the different inhibitor molecules on the metal surface and the synergistic effect of corrosion inhibition will disappear.

3.2. Potentiodynamic polarisation

To further analyse the anti-corrosion effect of the corrosion inhibitors on the 45 steel, polarisation curves of the samples were obtained. The polarisation curves were based on the open circuit potential of the electrode in the corrosion system (3.5% NaCl solution). The curves were obtained by scanning at 0.5 $mV \cdot s^{-1}$ in the range of ± 0.5 V. The polarisation curves and the electrochemical parameters obtained by fitting the polarisation curves enabled the mechanism of electrochemical corrosion to be further analysed and the corrosion inhibitory effect of the corrosion inhibitors to be evaluated[19].
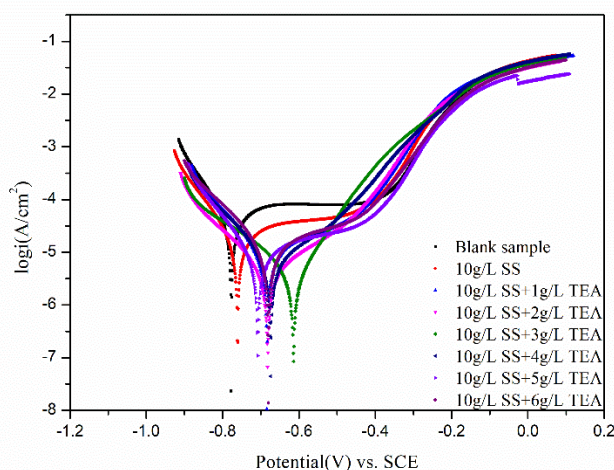
Figure 4. Polarisation curves of the samples measured in 3.5% NaCl solution.

Figure 4 shows the linear polarisation curves in 3.5% NaCl solution of the 45 steel blank sample, the samples coated with sodium silicate corrosion inhibitor and the six samples coated with the composite corrosion inhibitor containing different amounts of triethanolamine. The resulting polarisation curves were fitted and the results are shown in Table 2; E_{corr} is the self-corrosion potential, i_{corr} and i_{corri} are the self-corrosion current densities of the blank sample and the corrosion inhibitor coated sample, respectively, β_c and β_a are the cathode and anode slopes, respectively, and η is the corrosion current density protection efficiency calculated by equation (1)[20,21]. Generally, the smaller

the current density of the self-corrosion current, the better the corrosion resistance of the protective film[22].

$$\eta_{Tafel} = \frac{i_{corr} - i_{corri}}{i_{corr}} \times 100\% \qquad (1)$$

Table 2. Electrochemical parameters obtained from potentiodynamic polarization

Concentration ratios	E_{corr} (V vs. SCE)	β_c (V·decade^{-1})	β_a (V·decade^{-1})	i_{corr} (A·cm^{-2})	h (%)
Blank sample	-7.77×10^{-1}	-10.70×10^{-2}	3.81×10^{-2}	50.68×10^{-6}	–
10 g·L^{-1} SS	-7.60×10^{-1}	-9.61×10^{-2}	3.89×10^{-2}	20.68×10^{-6}	59.19
0 g·L^{-1} SS + 1 g·L^{-1} TEA	-6.84×10^{-1}	-8.04×10^{-2}	4.09×10^{-2}	10.82×10^{-6}	78.65
10 g·L^{-1} SS + 2 g·L^{-1} TEA	-6.82×10^{-1}	-7.09×10^{-2}	4.58×10^{-2}	9.44×10^{-6}	81.38
10 g·L^{-1} SS + 3 g·L^{-1} TEA	-6.14×10^{-1}	-6.22×10^{-2}	9.90×10^{-2}	3.50×10^{-6}	93.10
10 g·L^{-1} SS + 4 g·L^{-1} TEA	-6.74×10^{-1}	-8.48×10^{-2}	4.91×10^{-2}	7.91×10^{-6}	84.33
10 g·L^{-1} SS + 5 g·L^{-1} TEA	-7.08×10^{-1}	-9.10×10^{-2}	3.53×10^{-2}	9.70×10^{-6}	50.86
10 g/L SS+6g/L TEA	-6.80×10^{-1}	-7.66×10^{-2}	3.26×10^{-2}	13.25×10^{-6}	73.86

　　　　As shown in Table 2, the self-corrosion potential of the blank sample was –0.777 V, which was lower than that of the samples coated with corrosion inhibitors. The self-corrosion current density of the blank sample was 50.68×10^{-6} A·cm^{-2}, which was much higher than for the other samples. This indicated that the presence of corrosion inhibitors could effectively decrease the corrosion tendency of 45 steel from a thermodynamic and a dynamic point of view. When sodium silicate alone was used to form the corrosion inhibitory film, the self-corrosion current density decreased to 20.68×10^{-6} A·cm^{-2} and the self-corrosion potential was –0.760V, indicating that sodium silicate had a corrosion inhibitory effect. As the amount of triethanolamine that was added to the sodium silicate solution increased, the self-corrosion potential became even more positive and the self-corrosion current density further decreased. As the amount of triethanolamine reached 3 g·L^{-1}, the self-corrosion potential was –0.614 V, and the self-corrosion current density decreased to the lowest value of 3.5×10^{-6} A·cm^{-2}. In this case, the composite corrosion inhibitor had the best corrosion inhibitory effect. As the concentration of triethanolamine increased further, the self-corrosion potential no longer continued to positively shift and the self-corrosion current density began to increase. This indicated that the corrosion inhibitory effect of the composite corrosion inhibitor deteriorated as the amount of triethanolamine continued to increase.

　　　　The reason for this phenomenon was that insoluble silicate, which formed by the reaction of sodium silicate with metal ions on the surface of the sample, accumulated on the surface of the samples and inhibited the anode and cathode reactions. When triethanolamine was added to the sodium silicate solution to form a composite corrosion inhibitor, the self-corrosion potential was markedly positively shifted and the current density is also significantly decreased. This was because the protective film formed by the aggregation of silicate on the metal surface was non-homogeneously distributed and had local defects; the addition of triethanolamine as an adsorbent corrosion inhibitor filled these defects, thereby having a synergistic adsorption effect that made the protective film tighter. The obvious positive shift in the self-corrosion potential also showed that there was greater inhibition of the dissolution reaction in the anode zone than in the cathode zone. The composite corrosion inhibitor had the best corrosion inhibitory effect when the amount of triethanolamine reached 3 g·L^{-1} in sodium silicate, with a protection efficiency of 93.10%. However, as the concentration of triethanolamine further increased,

the corrosion inhibitory effect of the composite corrosion inhibitor deteriorated. This was because the concentration of triethanolamine was too high, transforming the synergistic adsorption process into competitive adsorption. Under the synergistic corrosion inhibition effect of triethanolamine and sodium silicate, the best combination of triethanolamine and sodium silicate (10 g·L^{-1} sodium silicate + 3 g·L^{-1} triethanolamine) has a corrosion inhibition efficiency of 93.1%, which was far superior to the corrosion inhibition efficiency of triethanolamine alone (69.9%)[23] or sodium silicate alone (60%)[24], and even more than that the best reported combination of traditional compounds sodium nitrite and triethanolamine inhibitor (82.3%) with 1000 ppm sodium nitrite + 2500 ppm triethanolamine[25].

3.3. Electrochemical impedance spectroscopy

To further study the influence of the corrosion inhibitors on the corrosion resistance of 45 steel and the underpinning mechanism, electrochemical impedance spectroscopy (EIS) was performed[26].
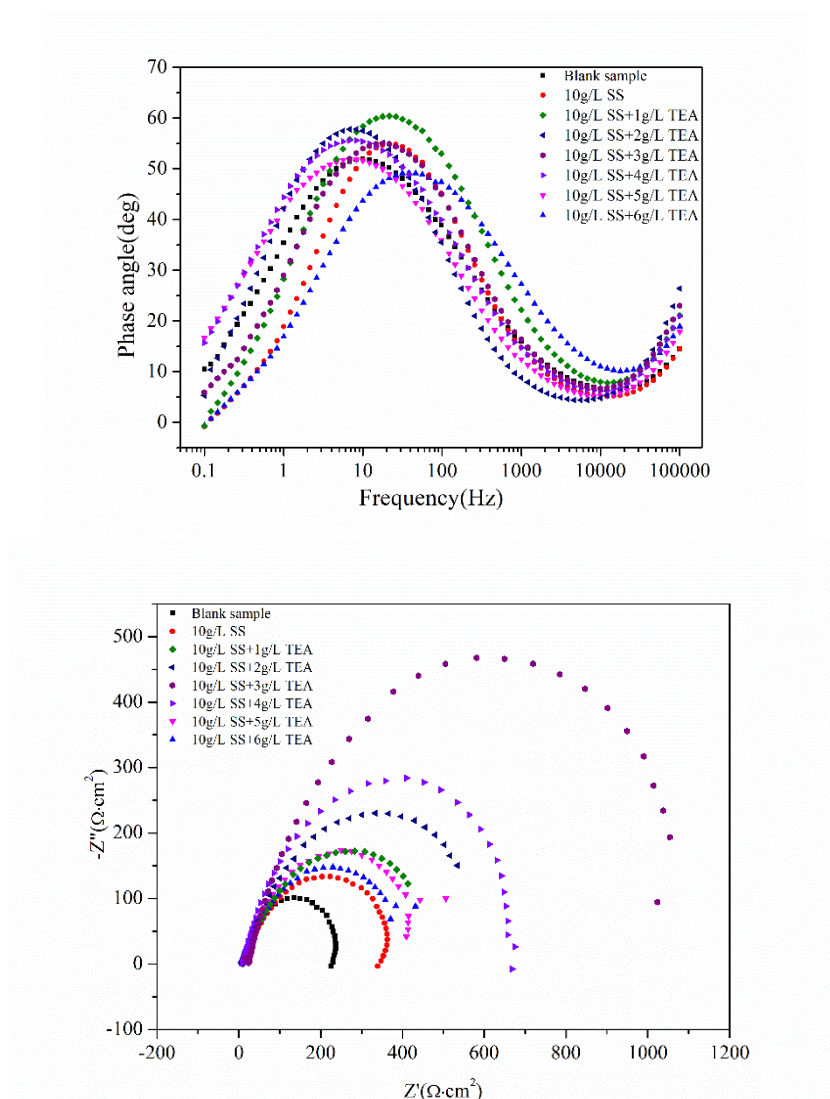
Figure 5. (a) Bode diagrams and (b) Nyquist diagrams for the samples in 3.5% NaCl solution.

Figure 6. Equivalent circuit model for EIS

Table 3. Fitting EIS parameters of the samples

	R_s ($\Omega \cdot cm^2$)	Q ($s^n \cdot \Omega^{-1} \cdot cm^{-2}$)	n	R_{ct} ($\Omega \cdot cm^2$)
Blank sample	8.92	3.55×10^{-3}	0.801	250.4
10 g·L^{-1} SS	9.41	2.90×10^{-3}	0.690	399.8
10 g·L^{-1} SS + 1 g·L^{-1} TEA	8.29	9.76×10^{-3}	0.698	553.5
10 g·L^{-1} SS + 2 g·L^{-1} TEA	7.74	7.45×10^{-3}	0.718	713.5
10 g·L^{-1} SS + 3 g·L^{-1} TEA	8.91	2.52×10^{-3}	0.795	1220
10 g·L^{-1} SS + 4 g·L^{-1} TEA	9.10	2.19×10^{-3}	0.787	736.6
10 g·L^{-1} SS + 5 g·L^{-1} TEA	9.81	4.02×10^{-3}	0.749	489.4
10 g·L^{-1} SS + 6 g·L^{-1} TEA	8.06	7.80×10^{-3}	0.695	473.7

It can be seen from Figure 5 that the samples exhibited similar impedance characteristics and one time constant. The equivalent circuit obtained by fitting the EIS spectra is shown in Figure 6, where R_s is the uncompensated resistance of the electrolyte and R_{ct} is the charge transfer resistance [27,28]. CPE is a constant phase angle element[29]. The fitting circuit parameters are shown in Table 3.

It can be seen from Table 3 that the charge transfer resistance of 45 steel coated with the sodium silicate corrosion inhibitor and sodium silicate triethanolamine composite corrosion inhibitors were all larger than that of uncoated corrosion inhibitor. Additionally, the charge transfer resistance values of the 45 steel samples coated with composite corrosion inhibitor were larger than that of the sample coated with just sodium silicate corrosion inhibitor. As the concentration of triethanolamine in the composite corrosion inhibitor increased, the charge transfer resistance value of the 45 steel gradually increased, reaching a maximum of 1220 $\Omega \cdot cm^{-2}$ when the concentration of triethanolamine was 3 g·L^{-1}. This was higher than the previously reported optimal combination of polyamidoamine dendrimers and sodium silicate of 1050 $\Omega \cdot cm^{-2}$[30]. Then, as the concentration of triethanolamine further increased, the charge transfer resistance continued to decrease.

Additionally, the phase angle increased after the addition of inhibitors, which was ascribed to the increase in the homogeneity of the surface that resulted from the adsorption of inhibitor molecules on the steel surface[31,32]. This showed that the composite corrosion inhibitor could effectively inhibit the corrosion of the 45 steel in sodium chloride solution, which was due to the adsorption and deposition of insoluble silicate formed by the reaction of sodium silicate and the surface metal on the 45 steel surface to form a relatively dense film. The addition of triethanolamine to sodium silicate resulted in synergistic adsorption, with triethylamine filling the defects in the protective surface film and thereby decreasing the number of defects and making the film more compact. This effectively inhibited the dissolution of

45 steel in the sodium chloride solution and the cathodic hydrogen evolution process. Therefore, as the amount of triethanolamine in the composite corrosion inhibitor increased, the charge transfer resistance of the 45 steel sample increased. When the addition of triethanolamine exceeded 3 g·L^{-1}, too much triethanolamine was adsorbed on the surface of the 45 steel and sodium silicate could not fully react with the metal surface to form a dense surface film; thus, the synergistic adsorption effect declined. In summary, the synergistic adsorption effect was optimal when 3 g·L^{-1} triethanolamine and 10 g·L^{-1} sodium silicate were used, which was consistent with all of the preceding results.

3.4. molecular simulation

In recent years, molecular simulation technology has been used to reveal information about the molecular structure and electronic distribution of corrosion inhibitors[33,34]. However, the mutual promotion of different corrosion inhibitor molecules has rarely been studied. Accordingly, the molecular structure of sodium silicate and triethanolamine was studied by molecular simulation and the synergistic process by which sodium silicate and triethanolamine molecules exerted their mutual promotion effect was simulated. The molecular structure models of sodium silicate and triethanolamine molecules are shown in Figure 7. DMOI3 in Material Studio was used to calculate the adsorption characteristics of the sodium silicate and triethanolamine molecules[35]. First, the structure of each molecule was optimised using the B3LYP method with medium precision, which was employed to calculate the single point energy[36]. From this, the energy gap ΔE (E_{HOMO}-E_{LUMO}) was calculated, where E_{HOMO} is the energy level of the highest occupied orbital energy of the molecule and E_{LUMO} is the energy level of the lowest unoccupied orbital energy. The magnitude of ΔE directly reflects the activity of the molecule in the environment: the larger the ΔE, the more stable the molecule and the less likely it is to react with other substances; conversely, the smaller the ΔE, the more likely it is to undergo chemical interactions with other substances.
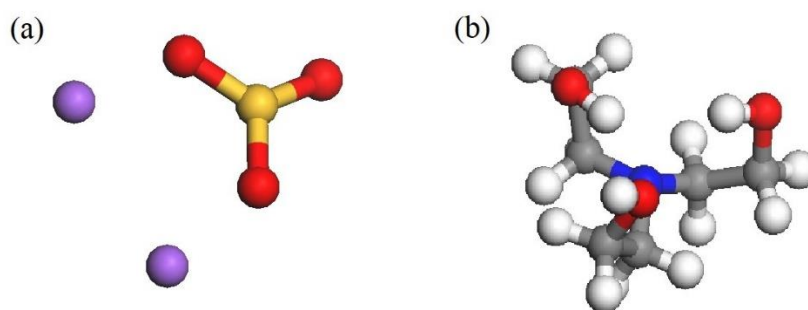
Figure 7. Molecular models of (a) sodium silicate and (b) triethanolamine molecule.

Table 4. The calculated molecular energy gap

Inhibitors	E_{HOMO}(eV)	E_{LUMO}(eV)	ΔE(eV)
SS	-3.191	-1.683	-1.508
TEA	-6.071	1.459	-7.53

It can be seen from Table 4 that the energy gap of the triethanolamine molecule was significantly larger than that of the sodium silicate molecule. This meant that the triethanolamine molecule was relatively stable and not prone to chemical adsorption. According to the results of the humidity and temperature accelerated corrosion testing and electrochemical measurements, the addition of triethanolamine improved the corrosion inhibitory effect of sodium silicate. To further study the mechanism underpinning this effect of triethanolamine, Fe atoms were chosen as the adsorption surface, calculation models with the sodium silicate molecule and different proportions of triethanolamine molecules were built, and the interaction energy of the models was calculated.

The splicing calculation model was built using the Build Layer function in Material Studio. The lower layer was the Fe atomic layer and the upper layer comprised sodium silicate and triethylamine molecules in different proportions, which were as close as possible to the molar ratios in the humidity and temperature accelerated corrosion test. The total number of molecules was fixed at 11. The initial structural model was optimised with the Force function and then molecular dynamics simulations were performed in the NVT system to calculate the interaction force between the molecular layer and the Fe atomic layer.
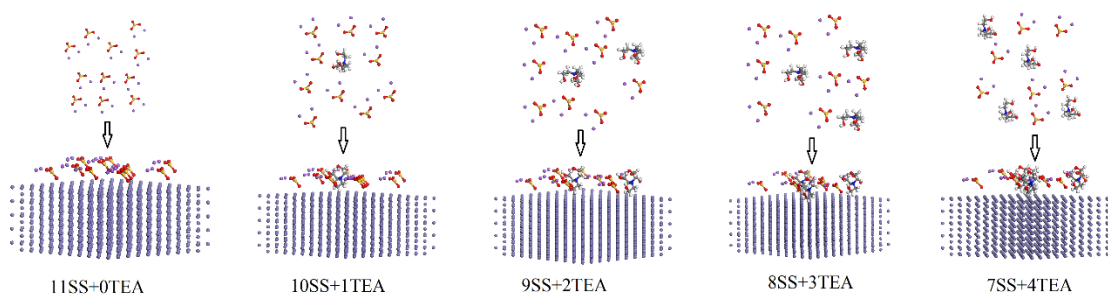
Figure 8. Build process of the molecular model

Figure 8 shows the build process of the model. The interaction energy between the corrosion inhibitor molecules and the surface Fe atoms was calculated according to equation (2).

$$E_{interaction} = E_{total} - (E_{molecule} + E_{surface}) \qquad (2)$$

Here, $E_{interaction}$ is the interaction energy, $E_{molecule}$ is the energy of the etchant molecular layer and $E_{surface}$ is the energy of the surface layer. The calculation results are shown in Table 5.

Table 5. The calculated energy of the molecular model

Molecular counts	E_{total}(KJ/mol)	$E_{molecule}$(KJ/mol)	E_{suface}(KJ/mol)	$E_{interaction}$(KJ/mol)
11SS+0TEA	-1026.77	-701.03	-7.02	-318.72
10SS+1TEA	-1038.50	-708.64	-7.02	-322.84
9SS+2TEA	-1020.75	-681.60	-7.02	-332.13
8SS+3TEA	-985.00	-656.32	-7.02	-321.66
7SS+4TEA	-932.50	-605.42	-7.02	-320.06

The interaction energy reflects the difficulty of adsorption of the corrosion inhibitor molecules on the Fe surface. The greater the interaction energy, the stronger the force between the molecular layer and the Fe surface; in other words, the easier it is to adsorb on the Fe surface. It can be seen from Table 5 that when the molar ratio of sodium silicate to triethanolamine was 9:2, the interaction force between the molecular layer and the Fe surface was the strongest. Interestingly, this ratio was the closest to 10gSS+3gTEA in the humidity and temperature accelerated corrosion test. Additionally, as the ratio of triethanolamine gradually increased, the interaction energy gradually decreased. This was consistent with the results of the humidity and temperature acceleration corrosion tests and the electrochemical measurements.

4. CONCLUSIONS

In this work, humidity and temperature accelerated corrosion testing combined with macroscopic observation, SEM and laser confocal microscopy and electrochemical measurements were adopted to study the corrosion inhibitory effect on 45 steel of sodium silicate corrosion inhibitor and composite corrosion inhibitors composed of different amounts of triethanolamine in sodium silicate solution. Molecular simulation was also used to study the synergistic adsorption effect of sodium silicate and triethanolamine. The results showed that the sodium silicate solution had a certain corrosion inhibitory effect on 45 steel but the resulting protective film was not dense enough, containing many defects. When triethanolamine was added to the sodium silicate solution it was adsorbed on the defects in the film formed by sodium silicate on the metal surface, making the surface film more stable, dense and complete. There was a synergistic adsorption effect between triethanolamine and sodium silicate. However, this synergistic adsorption effect did not continue indefinitely as the amount of triethanolamine increased. Initially, as the amount of triethanolamine increased, the synergistic adsorption effect gradually strengthened and was optimal at 3 g·L^{-1}, resulting in the optimal corrosion inhibitory effect. As the amount of triethanolamine continued to increase, competitive adsorption occurred between triethanolamine and sodium silicate and the corrosion inhibitory effect of the corrosion inhibitor decreased.

References

1. P. Bothi, R. Mathur and G. Sethuraman, *Mater. Lett.*, 62 (2008) 113.
2. J.J. Fu, S.N. Li, L.H. Cao, Y. Wang, L.H. Yan, L.D. Lu, *J. Mater. Sci.*, 45 (2010) 979.
3. A.G. Jorge, E.V. Araceli, R.R. Mario, U. C. Jorge and P.P. Manuel, *Arabian J. Chem.*, 12 (2019) 3244.
4. E. A. Florez-Frias, V. Barba, R. Lopez-Sesenes, L. L. Landeros-Martínez, J. P. Flores-De los Ríos, M. Casales, and J. G. Gonzalez-Rodriguez, *Int. J. Corros.*, 2021(2021) 1.
5. M. Abdallah, R. El-Sayed, A. Meshabi and M. Alfakeer, *Prot. Met. Phys. Chem.*, 57 (2021) 389.
6. M. Atik, P. de Lima Neto, L. A. Avaca, M. A. Aegerter and J. Zarzycki, *J. Mater. Sci. Lett.*, 13 (1994) 1081.
7. K.M. Eddine, I. Rachid, M.A. Bennouna, A. Aityoub, A. Abdesselam and A. Benyaich, *Corros. Rev.*, 39 (2021) 137.
8. M.F. Heragh and H. Tavakoli, *Met. Mater. Int.*, 26 (2019) 1654.
9. X. Wang, *Int. J. Electrochem. Sci.*, 15 (2020) 1606.
10. S. Chen, B. Zhu and X. Liang, *Int. J. Electrochem. Sci.*, 15 (2020) 1.
11. A. M. Resen, M. M. Hanoon, W. K. Alani, A. Kadhim, A. A. Mohammed, T. S. Gaaz, A. A. H. Kadhum, A. A. Al-Amiery and M. S. Takriff, *Int. J. Corros. Scale Inhib.*, 10(2021) 368.
12. S. C. Nwanonenyi, H. C. Obasi, E. E. Oguzie, I. C. Chukwujike and C. K. Anyiam, *J. Bio- Tribo-Corros.*, 3 (2017) 1.
13. S. Andreani, M. Znini, J. Paolini, L. Majidi, B. Hammouti, J. Costa and A. Muselli, *J. Mater. Environ. Sci.*, 7 (2016) 187.
14. R.D. Armstrong, L. Peggs and A. Walsh, *J. Appl. Electrochem.*, 24 (1994) 1244.
15. O. Lopez-Garrity and G. S. Frankel, *Electrochim. Acta*, 130 (2014) 9.
16. H. Gao, Q. Li, Y. Dai, F. Luo and H.X. Zhang, *Corros. Sci.*, 52 (2010) 1603.
17. G. Batis, P. Pantazopoulou and A. Routoulas, *Anti-Corros. Methods Mater.*, 48 (2001) 107.
18. O. Taeri, A. Hassanzadeh and F. Ravari, *ChemElectroChem.*, 7 (2020) 2123.
19. A. Adeyinka and B. Aremu, *ARPN J. Eng. and Appl. Sci.*, 7 (2012) 561.
20. J. Abdurrahman, D. Wahyuningrum, S. Achmad and B. Bundjali, *Sains Malays.*, 40 (2011) 973.
21. 21.R. Raj, Y. Morozov, L.M. Calado, M.G. Taryba, R. Kahraman, A. Shakoor and M.F. Montemor, *Electrochim. Acta*, 319 (2019) 801.
22. M. Lebrini, M. Lagrenée, H. Vezin, M.Traisnel and F. Bentiss, *Corros. Sci.*, 49 (2007) 2254.
23. M. Zhang and Y. Long, Inhibition of Triethanolamine for Magnetic Refrigeration Material LaFe11.0Co0.7Si1.3 in Distilled Water, *The 7th National Conference on Functional Materials and Applications*, Changsha, China, 2010, 1706.
24. K.S. Bokati, C. Dehghanian and S. Yari, *Corros. Sci.*, 126 (2017) 272.
25. K.T. Kim, H.Y. Chang, B.T. Lim, H.B. Park and Y. S. Kim, *Adv. Mater. Sci. Eng.*, 2016 (2016) 1.
26. D.A. López, S.N. Simison and S.R. de Sánchez, *Electrochim. Acta*, 48 (2003) 845.
27. E.V. Araceli, G.G. Sergio and R.G. Javier, *J. Anal. Bioanal. Tech.*, 6 (2015) 273.
28. S. Harisha, J. Keshavayya, B.E. Kumara Swamy, S.M. Prasanna, C.C. Viswanath and B.N. Ravi,
29. *J. Mol. Liq.*, 271 (2018) 976.
30. Y.J. Tan, S. Bailey and B. Kinsella, *Corros. Sci.*, 38 (1996) 1545.
31. B. Zhang, C. He, X. Chen, Z. Tian and F. Li, *Corros. Sci.*, 90 (2015) 585.
32. K. Zhang, W. Yang, X. Yin, Y. Chen, , Y. Liu, J. Le and B. Xu, *Carbohydr. Polym.*, 181 (2018) 191.

33. K. Zhang, W. Yang and B. Xu, *J. Colloid Interface Sci.*, 517 (2018) 52.
34. G. Gece, *Corros. Sci.*, 50 (2008) 2981.
35. I.H. Ali, *Mol.*, 26 (2021) 3679-3695.
36. A. Singh, K.R. Ansari, M.A. Quraishi and H. Lgaz, *Mater.*, 12 (2018) 1.
37. M. Ramezanzadeh, G. Bahlakeh, Z. Sanaei and B. Ramezanzadeh, *Appl. Surf. Sci.*, 463(2019) 1058.